

TPRU: ADVANCING TEMPORAL AND PROCEDURAL UNDERSTANDING IN LARGE MULTIMODAL MODELS

000
001
002
003
004
005 **Anonymous authors**
006 Paper under double-blind review
007
008
009
010

ABSTRACT

011 Multimodal Large Language Models (MLLMs), particularly smaller, deployable
012 variants, exhibit a critical deficiency in understanding temporal and procedural vi-
013 sual data, a bottleneck hindering their application in real-world embodied AI. This
014 gap is largely caused by a systemic failure in training paradigms, which lack large-
015 scale, procedurally coherent data. To address this problem, we introduce TPRU, a
016 large-scale dataset sourced from diverse embodied scenarios such as robotic ma-
017 nipulation and GUI navigation. TPRU is systematically designed to cultivate tem-
018 poral reasoning through three complementary tasks: Temporal Reordering, Next-
019 Frame Prediction, and Previous-Frame Review. A key feature is the inclusion of
020 challenging negative samples, compelling models to transition from passive ob-
021 servation to active, cross-modal validation. We leverage TPRU with a reinforce-
022 ment learning (RL) fine-tuning methodology, specifically targeting the enhance-
023 ment of resource-efficient models. Experiments show our approach yields dra-
024 matic gains: on our manually curated TPRU-Test, the accuracy of TPRU-7B soars
025 from 50.33% to 75.70%, a state-of-the-art result that significantly outperforms
026 vastly larger baselines, including GPT-4o. Crucially, these capabilities generalize
027 effectively, demonstrating substantial improvements on established benchmarks.
028 We will release our dataset and models to the community.
029

1 INTRODUCTION

030 Multimodal Large Language Models (MLLMs) have demonstrated impressive capabilities, with
031 leading large-scale open-source (Bai et al., 2025; Zhu et al., 2025) and proprietary models (Hurst
032 et al., 2024) achieving remarkable performance on a wide range of vision-language tasks. However,
033 this progress masks a critical and widening gap: while massive, expensive models show emerging
034 competence, their smaller and more efficient counterparts struggle profoundly with complex reason-
035 ing. Especially when they try to understand temporal and procedural image sequences (Song et al.,
036 2025; Tang et al., 2025; Zhang et al., 2025). This capability gap is not merely an academic concern
037 but a primary obstacle hindering the deployment of MLLMs in real-world and interactive applica-
038 tions. Downstream tasks like robotic manipulation, embodied navigation, and instruction following
039 often operate on resource-constrained edge devices where deploying dozens or hundreds billion pa-
040 rameter models is infeasible (Ji et al., 2025; Lu et al., 2024; Savva et al., 2019). Consequently,
041 the inability of small models to grasp state changes and procedural logic represents a fundamental
042 bottleneck for the entire field of embodied AI.
043

044 The root of this deficiency lies not in model scale alone, but in a systemic failure of the prevailing
045 training paradigm. Existing paradigms predominantly focus on aligning text with a single image (Li
046 et al., 2023) or treating multiple images as an unordered collection (Jiang et al., 2024). **Although**
047 **datasets like LLaVA-NeXT-Interleave (Li et al., 2024) incorporate multi-frame inputs derived from**
048 **videos, they primarily emphasize general sequential content comprehension rather than the fine-**
049 **grained temporal and procedural understanding.** This approach overlooks the critical distinction
050 between understanding a set of images and comprehending a sequence of images. As shown in Fig-
051 ure 1(a), the community’s response has been to create evaluation-only benchmarks that repeatedly
052 confirm this failure (Wang et al., 2024; Tang et al., 2025), rather than addressing the root cause,
053 which is the absence of large-scale, high-quality real-world sequential data for training. This over-
sight stems from the inherent difficulty of capturing the complex, continuous transformations of

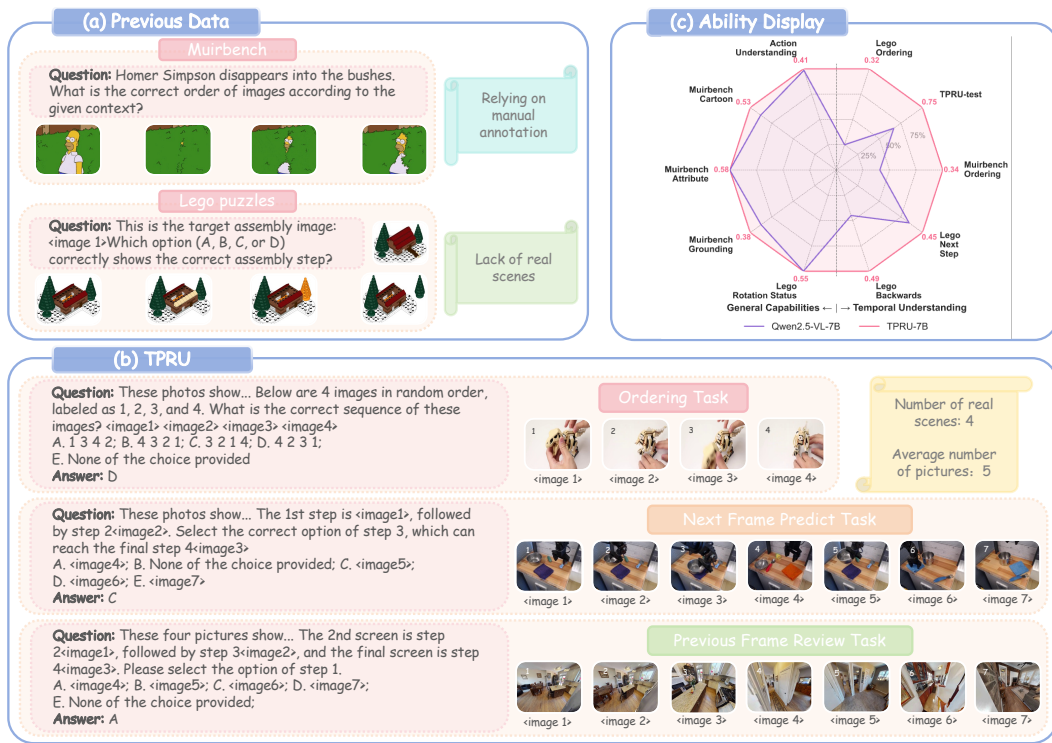


Figure 1: An overview of our TPRU dataset. Unlike prior synthetic datasets (a), TPRU is built from real-world scenarios and structured into temporal tasks (b). As shown in the ability display (c), TPRU-7B achieves significant performance gains in temporal understanding.

real-world actions. As a result, smaller models are evaluated on a sophisticated skill they were never systematically taught, leading to poor performance in detecting procedural errors and leaving genuine procedural understanding an unsolved problem for deployable AI systems (Song et al., 2025; Fu et al., 2024a).

To bridge this critical capability gap, particularly for resource-constrained models, we introduce TPRU (Temporal-Procedural Understanding dataset), a novel dataset designed to bridge the gap between evaluation and training. First, to address data scarcity and authenticity, TPRU provides a large-scale training set (24,750 QA pairs, 126,000 images) sourced from four diverse and authentic embodied scenarios: robotic manipulation, embodied navigation, mobile GUI interaction, and LEGO assembly. More importantly, as depicted in Figure 1(b), TPRU is not just a data collection but a systematically structured dataset designed to cultivate a deep procedural understanding through three complementary task formats: **Temporal Reordering**, **Next-Frame Prediction** and **Previous-Frame Review**. To ensure models develop true comprehension beyond superficial heuristics, TPRU incorporates a significant number of challenging negative samples with deliberate inconsistencies, forcing models to transition from passive "seeing" to active validation. To benchmark this capability, we also present the TPRU-Test, a manually curated set of 461 challenging instances for rigorous evaluation.

Leveraging our TPRU dataset, we employed a reinforcement learning (RL) strategy to fine-tune a suite of Qwen2.5-VL models, focusing on smaller parameter counts. The results are striking. Our RL-finetuned models not only show massive improvements over their base versions but also significantly outperform existing state-of-the-art (SOTA) MLLMs on our proposed TPRU test set. Remarkably, our TPRU-7B and TPRU-32B surpass the performance of the much larger proprietary model GPT-4o and large-scale open-source models. Furthermore, as shown in Figure 1(c), TPRU-7B exhibits substantial gains on established multi-image benchmarks like MuirBench (Wang et al., 2024) and LEGO-Puzzles (Tang et al., 2025). These findings demonstrate that the temporal reasoning gap in small models is not an inherent limitation of their scale but a solvable challenge of

108 targeted data and training. We have unlocked SOTA-level procedural understanding in models small
 109 enough for practical, real-world deployment. Our contributions are summarized as below:
 110

- 111 • We construct TPRU, a new, large-scale, high-quality multi-image dataset focused on fine-
 112 grained temporal and procedural understanding, designed to empower smaller models for
 113 embodied contexts. The dataset and its creation methodology will be publicly released.
- 114 • We present a challenging held-out test set, TPRU-Test, manually curated and verified to
 115 rigorously evaluate temporal understanding in MLLMs.
- 116 • We propose and validate an effective reinforcement learning-based training methodology
 117 that enables small-to-medium-sized MLLMs to achieve and even surpass the temporal un-
 118 derstanding capabilities of vastly larger models. Extensive experiments demonstrate this
 119 superiority and strong generalization on both our TPRU-test and existing public bench-
 120 marks.

122 2 RELATED WORK

124 While Multimodal Large Language Models (MLLMs) excel at single-image comprehension (Fu
 125 et al., 2024a; Zhang et al., 2024a), reasoning across multiple images remains a significant challenge.
 126 To address this limitation, recent work has moved beyond the single-frame paradigm to tackle more
 127 complex real-world tasks (Wang et al., 2025b). This emerging research direction has necessitated
 128 the development of specialized instruction-tuning datasets and rigorous evaluation benchmarks.

130 2.1 MULTI-IMAGE TRAINING DATA

132 To enhance the multi-image capabilities of Multimodal Large Language Models (MLLMs), re-
 133 searchers have constructed large-scale instruction-tuning datasets. For instance, Mantis-Instruct
 134 (Jiang et al., 2024) adopts a skill-oriented strategy, efficiently imbuing models with four core abili-
 135 ties via a meticulously constructed 721K-sample dataset. LLaVA-NeXT-Interleave (Li et al., 2024)
 136 advances this direction by leveraging its 1.18M-sample M4-Instruct dataset and a unified interleaved
 137 data format to seamlessly handle multi-image, video, and 3D scenarios. Addressing conversational
 138 depth, MMDU (Liu et al., 2024) and MMCR (Yan et al., 2025) provide large-scale datasets specif-
 139 ically for training models on coherent reasoning in multi-turn dialogues. Furthermore, datasets
 140 have expanded into specific domains, such as RoboBrain’s ShareRobot (Ji et al., 2025), which pro-
 141 vides planning and affordance annotations for robotics tasks, and GUI Odyssey (Lu et al., 2024),
 142 which focuses on cross-application mobile device navigation. In parallel, innovative data genera-
 143 tion paradigms are emerging that move beyond reliance on manual annotation. Jigsaw-R1 (Wang
 144 et al., 2025c), for example, enhances models’ spatial awareness by programmatically generating
 145 jigsaw puzzle tasks for rule-based visual reinforcement learning. Taking this further, MiCo (Chen
 146 et al., 2025) proposes a fully self-supervised reinforcement learning framework, enabling models to
 147 learn complex reasoning from programmatically constructed contrastive image triplets without any
 148 instruction data.

149 While these datasets have significantly advanced multi-image instruction tuning, they often treat im-
 150 ages as an unordered collection. Even datasets with inherent sequentiality lack a systematic frame-
 151 work designed to teach the underlying principles of procedural flow. Our work addresses this gap
 152 by introducing TPRU. Through its complementary three temporal tasks, TPRU is specifically engi-
 153 neered to instill a foundational understanding of procedural dynamics.

154 2.2 BENCHMARKS FOR MULTI-IMAGE EVALUATION

155 Concurrently with the development of training data, a suite of rigorous benchmarks has been es-
 156 tablished to evaluate these emerging capabilities. For comprehensive and robust evaluation, Muir-
 157 Bench (Wang et al., 2024) presents a 2,600-question test whose key innovation is a pairwise de-
 158 sign—matching each answerable question with a minimally different, unanswerable variant to rig-
 159 orously test against hallucination. Targeting specific reasoning domains, STRIPCIPHER (Wang
 160 et al., 2025b) leverages wordless comic strips to assess narrative and temporal logic, while TempVS
 161 (Song et al., 2025) focuses on event ordering with a design that resists single-modality shortcuts. For
 162 spatial and physical reasoning, LEGO-Puzzles (Tang et al., 2025) creates a challenging testbed for

162 multi-step planning based on LEGO instructions, and MV-Math (Wang et al., 2025a) fills a critical
 163 gap in multi-visual context mathematical reasoning using real K-12 educational materials. Other
 164 benchmarks probe more fundamental visual abilities; BLINK (Fu et al., 2024b) aims to decouple
 165 core visual perception from linguistic reasoning, and MMRA (Wu et al., 2024) evaluates the ability
 166 to identify cross-image relations at multiple granularities. Finally, to systematize the application of
 167 these benchmarks, toolkits like VLMEvalKit (Duan et al., 2024) provide a standardized evaluation
 168 framework, greatly facilitating reproducible and comprehensive assessment across the community.

169 While invaluable for diagnosis, the critical limitation of these benchmarks is their evaluation-only
 170 nature, creating a disconnect between training and testing. TPRU bridges this gap by providing an
 171 integrated solution: a large-scale, structured training set alongside a challenging, manually curated
 172 test set to unify the development and evaluation of procedural understanding.

174 3 TPRU

176 While current Multi-modal Large Language Models excel on static single-image tasks, their performance
 177 degrades sharply as the number of input images increases (Li et al., 2024). This deficiency is
 178 exacerbated when processing image sequences that represent a coherent process or event. Recent
 179 work shows existing MLLMs largely fail to comprehend temporal dynamics and sequential relationships
 180 between visual frames. This limitation is starkly revealed on benchmarks for narrative comics,
 181 procedural instructions, and event ordering (Song et al., 2025; Tang et al., 2025; Wang et al., 2025b;
 182 2024). Consequently, the inability to grasp temporal dynamics severely hinders their applicability in
 183 real-world scenarios that demand comprehension of procedural activities and evolving states (Tang
 184 et al., 2025; Ji et al., 2025).

185 To systematically enhance and evaluate the capability of MLLMs in comprehending image sequences with temporal and procedural order, we propose the TPRU dataset. The dataset consists
 186 of two components. TPRU-25k is a fine-tuning set with 24,750 samples across four procedural scenarios,
 187 designed to enhance the model’s temporal and procedural understanding. TPRU-test is an
 188 evaluation benchmark comprising 461 manually annotated samples across five application scenarios.
 189 The detailed data sourcing and construction methodologies for TPRU-25k and TPRU-test are
 190 elaborated in Sections 3.1 and 3.2, respectively.

192 3.1 TPRU-25K

194 **Data Sources.** TPRU aims to provide MLLMs with high-quality, multi-image sequential data characterized by clear procedural and temporal structures. To construct a dataset with coherent procedural logic and ensure that the image sequences represent meaningful, ordered events, we sourced data from four diverse and complementary real-world scenarios: (1) **Robotic Manipulation.** Data is primarily derived from the “planning” tasks in the ShareRobot dataset (Ji et al., 2025), where we sample video frames to create discrete action sequences. (2) **LEGO Assembly.** Data is curated from 36 high-quality stop-motion videos from the YouTube creator Arvin Bricks, providing blur-free, state-distinct images ideal for part-to-whole reasoning. (3) **GUI Operation.** A novel dataset constructed from four-step screenshot sequences from GUI Odyssey (Lu et al., 2024) to capture goal-driven digital workflows. (4) **Embodied Navigation.** This category consists of ordered visual observations from agents navigating in simulated environments like Habitat (Savva et al., 2019). The diversity of these sources ensures the data is not confined to a single domain, fostering the development of generalizable sequential understanding.

207 **Generation Pipeline** Our data generation pipeline systematically transforms raw sequential data from diverse sources into structured training instances. The process involves three main stages: sequence filtering, text description generation, and task formulation, as illustrated in Figure 2.

210 **(a) Filtering and Quality Control.** Our dataset is constructed from heterogeneous sources, including temporally sampled video frames and ordered screenshots from embodied agent tasks and mobile UI interactions. We process these diverse inputs into a canonical format of coherent image sequences, each containing three to four images. To ensure high data quality and procedural integrity, every image sequence is subjected to a rigorous filtering pipeline. We employ Qwen2.5-VL-72B (Bai et al., 2025) as an automated quality assessor to discard sequences exhibiting visual blurriness, abrupt scene transitions, or a lack of discernible temporal progression. This stringent

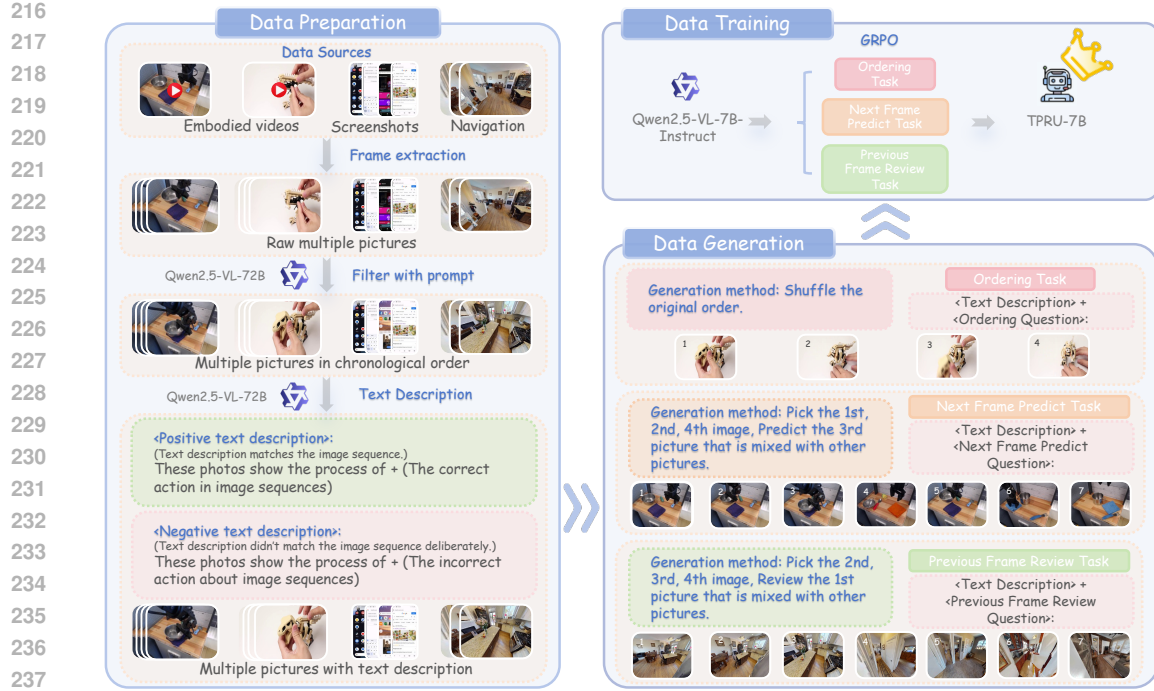


Figure 2: The TPRU dataset construction and training pipeline. Chronological image sequences from embodied sources are curated with both positive and negative text descriptions. These image sequences are then formulated into three tasks (Ordering, Next Frame Prediction, and Previous Frame Review) to fine-tune MLLMs for enhanced temporal and procedural understanding.

protocol guarantees that only high-fidelity, logically coherent sequences are used for subsequent processing.

(b) Description Generation and Robustness Enhancement. For each filtered image sequence, we generate a corresponding textual description using Qwen2.5-VL-72B to reinforce the model’s core vision-language alignment. To specifically bolster robustness and mitigate hallucination, we also introduce a negative sampling strategy. This involves creating a subset of instances where the textual description is deliberately mismatched with the visual content (e.g., pairing the instruction “pick up the fork” with images of “putting down a knife”). For these challenging cases, the target output is formulated as “None of the choices provided” (Wang et al., 2024). This forces the model to perform explicit cross-modal verification rather than relying solely on textual priors.

(c) Task Formulation. Based on the curated image sequences and their corresponding textual descriptions, we formulate three distinct yet complementary tasks designed to comprehensively enhance the model’s temporal and procedural understanding ability.

- **Temporal Ordering.** The primary objective of this task is to evaluate and enhance the model’s comprehension of an entire procedural timeline. We formulate this as a reordering problem. For a given image group, we shuffle the temporal order of the frames and provide the corresponding textual description. The model is then required to output the correct permutation that restores the reasonable sequence of the event.

- **Next Frame Prediction.** This task improves the model’s grasp of temporal coherence and procedural flow. The model is presented with the initial, second, and terminal frames of a four-frame procedural sequence and must select the correct intervening third frame from a set of candidates. These candidates include distractors from other similar scenarios. This task directly simulates the immediate planning required for robotic agents to anticipate the direct consequences of an action.

- **Previous Frame Review.** This task enhances the model’s ability to reconstruct the historical context of a procedural segment. The model is given the final three frames of a four-frame sequence and is tasked with identifying the correct initial frame from a set of candidates. This capability

270 improves the model’s understanding of procedural prerequisites and its ability to trace an observed
 271 event back to its origin, a fundamental aspect of comprehensive temporal understanding.
 272

273 Collectively, these three complementary tasks are engineered to advance MLLMs beyond static
 274 image analysis. By jointly addressing temporal ordering, forward prediction, and backward review,
 275 our approach endows the model with a more profound and structured comprehension of procedural
 276 dynamics, significantly enhancing its ability to interpret the temporal evolution of events depicted
 277 in image sequences.

278
 279 **3.2 TPRU-TEST**

280 To rigorously evaluate the temporal and procedural understanding capabilities of MLLMs, we in-
 281 troduce TPRU-Test, a dedicated, held-out evaluation set. TPRU-Test is meticulously curated and
 282 verified by human experts to ensure high quality and present novel generalization challenges. Its
 283 composition is deliberately diverse, incorporating the most demanding instances from our four
 284 core domains (Robotic Manipulation, LEGO Assembly, GUI Operation, and Embodied Naviga-
 285 tion) alongside complex, human activities from the EPIC-KITCHENS (Damen et al., 2020) dataset
 286 to probe model robustness. TPRU-Test inherits three complementary tasks of our training set, as-
 287 sessing temporal ordering, next-frame prediction, and previous-frame review. The curation protocol
 288 was exceptionally stringent. Each instance underwent a multi-stage human review where annotators
 289 picked and verified the ground-truth image sequence, authored plausible yet incorrect distractors,
 290 and ensured question clarity. Subsequently, every instance was cross-verified by at least one other
 291 expert to eliminate errors and subjective judgments. This process yields a high-quality benchmark
 292 of 461 instances across 5 distinct scenarios, engineered to provide a robust measure of genuine
 293 progress in temporal and procedural understanding for MLLMs.

294
 295 **4 EXPERIMENTS**
 296

297 In this section, we conduct comprehensive experiments to validate the effectiveness of our proposed
 298 TPRU dataset. We fine-tuned Qwen2.5-VL on TPRU-25k and evaluated on TPRU-test as well as on
 299 established public benchmarks. In Section 4.1, we assess the model’s performance on MuirBench
 300 (Wang et al., 2024) and LEGO-Puzzles (Tang et al., 2025) benchmarks which include tasks relevant
 301 to temporal and procedural understanding. And we present the primary results on our TPRU-test set
 302 in Section 4.2. To ensure our method does not degrade performance on broader tasks, we evaluate
 303 on general-purpose benchmarks in Section 4.3. Finally, in Section 4.4, we report a series of abla-
 304 tion studies to investigate the contribution of key components of our dataset. The hyperparameter
 305 Settings and reward designs of the experiment can be obtained respectively in Appendix A and F.
 306

307 **4.1 EVALUATION OF TEMPORAL RELATED BENCHMARKS**

308 **Performance on MuirBench.** As presented in Table 1, our TPRU-finetuned models demonstrate
 309 significant improvements over their Qwen2.5-VL base models across all scales on the MuirBench
 310 (Wang et al., 2024). Notably, our TPRU-32B model achieves an overall accuracy of 68.42%, out-
 311 performing the powerful proprietary model GPT-4o (68.00%) and closely matching the much larger
 312 Qwen2.5-VL-72B.

313 The most substantial gains are observed in the Ordering sub-task, which directly aligns with the
 314 temporal reasoning skills targeted by our TPRU dataset. TPRU-32B achieves a remarkable 45.31%
 315 in this category, drastically surpassing both its base model and GPT-4o. This trend is consistent
 316 across scales, with the score of TPRU-7B also more than doubling from 14.06% to 34.38%. Beyond
 317 temporal tasks, our training methodology enhances broader relational reasoning abilities, evidenced
 318 by significant improvements in tasks such as Difference Spotting and Visual Retrieval. These results
 319 confirm that our approach not only instills specialized temporal skills but also strengthens general
 320 cross-image reasoning capabilities.

321 **Performance on LEGO-Puzzles.** The efficacy of our approach is further validated on the LEGO-
 322 Puzzles benchmark, which directly evaluates procedural assembly reasoning as detailed in Table 2.
 323 Our models consistently outperform their base versions, with TPRU-7B achieving an overall score
 324 of 42.8%. This result confirms that the skills learned from our TPRU-25k dataset exhibit strong

324 **Table 1: Performance on MuirBench.** The light gray rows show the absolute improvement (in percentage
 325 points) of our models over their corresponding Qwen2.5-VL base models. **Gains** are shown in red, and **losses**
 326 in blue.

Model	Action Underst.	Attribute Similarity	Cartoon Underst.	Counting	Diagram Underst.	Difference Spotting	Geographic Underst.	Image-Text Matching	Ordering	Scene Underst.	Visual Grounding	Visual Retrieval	Overall
Open-source													
InternVL3-78B	48.17	61.73	44.87	50.85	83.17	55.59	60.00	79.31	31.25	69.35	44.05	66.10	64.65
InternVL3-38B	44.51	66.33	46.15	45.30	78.14	61.18	63.00	77.80	32.81	61.29	36.90	72.95	64.12
Qwen2.5-VL-72B	50.00	59.18	42.31	49.57	89.45	60.59	50.00	87.93	40.63	76.34	46.43	78.42	69.35
Qwen2.5-VL-32B	36.59	51.02	47.44	45.30	82.41	58.53	47.00	85.78	26.56	72.04	41.67	67.12	63.73
Qwen2.5-VL-7B	40.85	58.67	46.15	34.19	77.89	54.41	49.00	72.63	14.06	61.83	33.33	63.70	58.35
Qwen2.5-VL-3B	36.59	44.39	46.15	32.91	58.04	46.47	49.00	54.09	9.38	59.14	40.48	38.70	46.62
Proprietary													
Gemini-2.5-Flash	50.00	49.49	60.26	82.05	92.71	70.00	47.00	86.64	46.88	83.87	59.52	70.89	73.73
GPT-4o	44.51	56.12	51.28	49.15	88.69	60.29	56.00	86.85	23.44	71.51	36.90	80.14	68.00
Claude-3.5-Sonnet	35.37	55.10	44.87	35.90	76.38	54.12	41.00	77.59	25.00	54.84	47.62	57.53	57.69
Ours													
TPRU-32B	40.24	51.02	51.28	47.44	85.68	63.24	60.00	87.28	45.31	75.81	44.05	80.14	68.42
Improvement	+3.65	0.00	+3.84	+2.14	+3.27	+4.71	+13.00	+1.50	+18.75	+3.77	+2.38	+13.02	+4.69
TPRU-7B	41.46	57.65	47.44	34.62	82.91	63.82	63.00	82.11	34.38	67.74	38.10	75.68	65.04
Improvement	+0.61	-1.02	+1.29	+0.43	+5.02	+9.41	+14.00	+9.48	+20.32	+5.91	+4.77	+11.98	+6.69
TPRU-3B	39.63	51.02	47.44	40.17	67.34	55.88	84.00	68.32	23.44	72.04	53.57	66.10	59.31
Improvement	+3.04	+6.63	+1.29	+7.26	+9.30	+9.41	+35.00	+14.23	+14.06	+12.90	+13.09	+27.40	+12.69

344 positive generalization to complex, structured assembly tasks. The most pronounced improvements
 345 are concentrated in the Multi-Step Reasoning category, confirming the targeted impact of our training
 346 methodology. For the TPRU-7B, performance on the Ordering task quadruples, soaring from
 347 8.0% to 32.0%. Similarly, its capability in Backwards reasoning more than doubles, jumping from
 348 22.0% to 49.0%, and a significant gain is also observed in Next-Step sub-task. These enhancements
 349 strongly indicate that the procedural and causal reasoning abilities cultivated by the TPRU dataset
 350 effectively transfer to the logical, sequential challenges inherent in the LEGO-Puzzles.

351 **Table 2: Performance on LEGO-Puzzles.** The light gray rows show the absolute improvement (in percentage
 352 points) of our models over their corresponding Qwen2.5-VL base models. **Gains** are shown in red, and **losses**
 353 in blue.

Models	Height	Adjacency	Rotation	Multiview	Next-Step	Dependency	Rotation Stat.	Position	Backwards	Ordering	Outlier	Overall
Open-source												
InternVL3-78B	52.0	63.0	36.0	54.0	64.0	80.0	58.0	29.0	25.0	22.0	37.0	47.3
InternVL3-38B	40.0	60.0	39.0	55.0	57.0	81.0	59.0	33.0	47.0	12.0	36.0	47.2
Qwen2.5-VL-72B	43.0	58.0	38.0	39.0	57.0	76.0	57.0	52.0	74.0	43.0	43.0	52.7
Qwen2.5-VL-32B	35.0	60.0	38.0	52.0	45.0	79.0	51.0	45.0	66.0	43.0	43.0	50.6
Qwen2.5-VL-7B	20.0	57.0	32.0	47.0	38.0	67.0	56.0	29.0	22.0	8.0	25.0	36.5
Qwen2.5-VL-3B	29.0	55.0	30.0	36.0	32.0	65.0	48.0	19.0	16.0	4.0	25.0	32.6
Proprietary												
Gemini-2.5-Flash	52.0	58.0	37.0	55.0	58.0	74.0	53.0	49.0	40.0	46.0	29.0	50.1
GPT-4o	49.0	66.0	41.0	51.0	65.0	87.0	51.0	51.0	53.0	72.0	49.0	57.7
Claude-3.5-Sonnet	39.0	60.0	42.0	48.0	61.0	78.0	58.0	37.0	49.0	54.0	64.0	53.6
Ours												
TPRU-32B	34.0	61.0	35.0	47.0	55.0	76.0	52.0	48.0	70.0	49.0	48.0	52.3
Improvement	-1.0	+1.0	-3.0	-5.0	+10.0	-3.0	+1.0	+3.0	+4.0	+6.0	+5.0	+1.7
TPRU-7B	23.0	56.0	37.0	40.0	45.0	67.0	55.0	31.0	49.0	32.0	36.0	42.8
Improvement	+3.0	-1.0	+5.0	-7.0	+7.0	0.0	-1.0	+2.0	+27.0	+24.0	+11.0	+6.3
TPRU-3B	30.0	54.0	32.0	40.0	37.0	69.0	49.0	14.0	30.0	8.0	24.0	35.2
Improvement	+1.0	-1.0	+2.0	+4.0	+5.0	+4.0	+1.0	-5.0	+14.0	+4.0	-1.0	+2.6

4.2 EVALUATION OF GENERAL BENCHMARKS

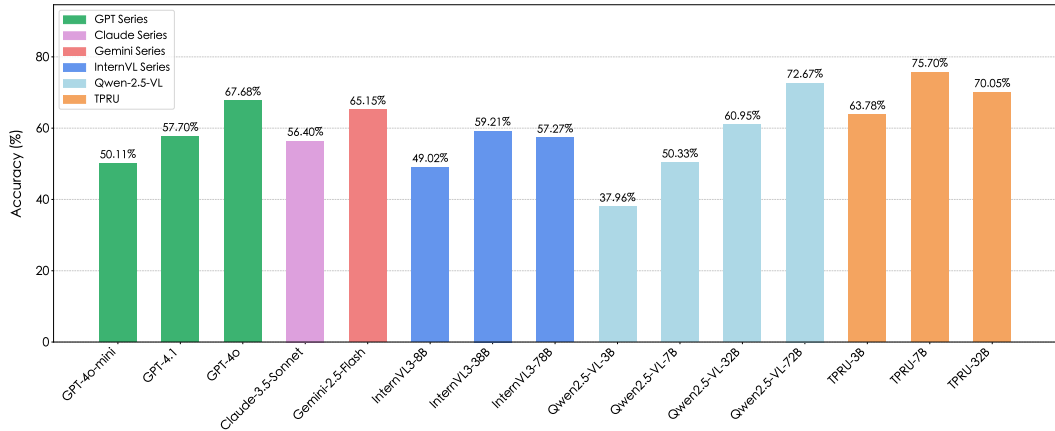
372 To ensure our specialized training does not degrade general capabilities, we evaluated our model on a
 373 range of broad multi-image benchmarks, as shown in Table 3. The results confirm that our finetuned
 374 models maintain or slightly improves performance across these diverse tasks. This pattern of stable
 375 to positive gains, such as on MMMU (+2.6) and MMCR (+1.08) for TPRU-7B, demonstrates that our
 376 method for enhancing temporal reasoning successfully avoids catastrophic forgetting and preserves
 377 the model’s foundational abilities. The relevant content of these benchmarks can be obtained from
 the appendix.

378
 379 **Table 3: Evaluation on general multi-image benchmarks.** Results show that our TPRU models maintain
 380 comparable performance to their base models, indicating that our specialized training does not degrade general
 381 capabilities.

382 Model	383 MME- RealWorld-Lite	384 BLINK	385 RealWorld QA	386 MMCR	387 MMTBench	388 MMStar	389 MMMU-Dev	390 Overall
Open-source								
385 InternVL3-78B	386 65.40	387 66.30	388 78.00	389 20.29	390 73.20	391 72.50	392 64.20	393 62.84
385 InternVL3-38B	386 67.30	387 64.49	388 75.60	389 21.38	390 71.80	391 71.50	392 62.00	393 62.01
385 Qwen2.5-VL-32B	386 45.96	387 59.34	388 68.89	389 37.32	390 58.89	391 54.93	392 34.67	393 51.43
385 Qwen2.5-VL-7B	386 44.55	387 54.76	388 68.10	389 22.83	390 61.46	391 61.67	392 44.40	393 51.11
385 Qwen2.5-VL-3B	386 41.94	387 48.97	388 65.36	389 19.20	390 60.47	391 54.40	392 44.67	393 47.86
Ours								
390 <i>TPRU-32B</i>	391 44.92	392 58.81	393 69.80	394 39.86	395 56.25	396 52.26	397 34.00	398 50.84
390 <i>TPRU-7B</i>	391 45.34	392 55.86	393 69.54	394 23.91	395 61.85	396 61.13	397 47.00	398 52.09
390 <i>TPRU-3B</i>	391 39.19	392 48.13	393 66.54	394 21.01	395 60.89	396 54.93	397 44.67	398 47.91

395 4.3 MAIN RESULTS ON TPRU-TEST

396 We evaluate the core efficacy of our approach on the proposed **TPRU-test**, a benchmark specifically
 397 designed to assess fine-grained temporal ordering, causal prediction, and procedural consistency.
 398 The results, presented in Figure 3, demonstrate that fine-tuning with our TPRU dataset with
 399 RL methodology yields substantial and consistent performance improvements across various model
 400 scales. Notably, the accuracy of TPRU-7B soars from 50.33% to **75.70%**, while the TPRU-3B shows
 401 a similarly strong improvement from 37.96% to **60.95%**. This level of performance is highly competitive:
 402 TPRU-7B surpasses the powerful proprietary model GPT-4o by a significant margin. These
 403 results unequivocally validate the effectiveness of our training paradigm. The dramatic performance
 404 gains underscore that targeted training on procedurally-grounded data, enriched with challenging
 405 negative samples and optimized via reinforcement learning, is a potent strategy for instilling robust
 406 sequential reasoning capabilities in MLLMs.



421 Figure 3: Performance of different models on TPRU-test.

424 4.4 ABLATION STUDIES

425 To systematically investigate the contributions of the core components of our methodology, we
 426 conducted a series of ablation studies. We evaluate the impact of task composition, negative samples
 427 and data volume. All experiments are conducted by training variants of the Qwen2.5-VL-7B model,
 428 with performance evaluated on MuirBench and Lego-Puzzles. The detailed results are presented in
 429 Appendix.

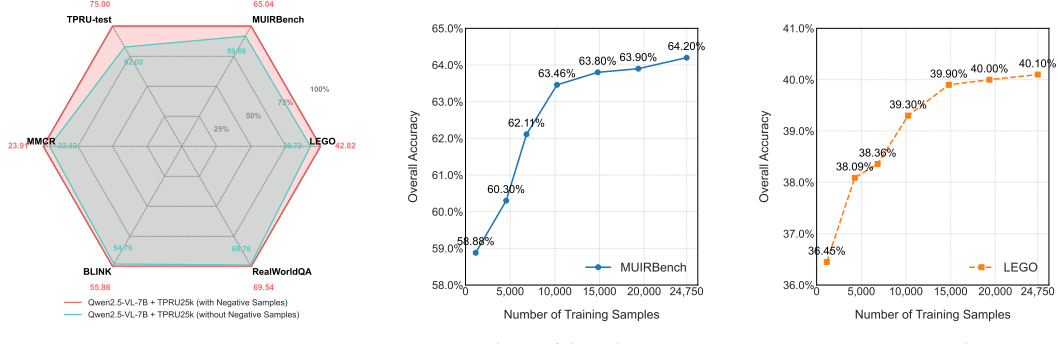
430 **Impact of Task Composition.** We conducted an ablation study on a small-scale dataset of 8,250
 431 samples to analyze the individual and combined contributions of our core training tasks, with results

432 Table 4: Ablation study on the effect of different TPRU data components for the **Qwen2.5-VL-7B**
 433 model on MuirBench and LEGO-Puzzles benchmarks. The inclusion of a component is marked
 434 with a \checkmark . All scores are Overall Accuracy (%). The volume of data remains consistent.

TPRU Data Components			Benchmark Accuracy (%)	
Ordering	Previous Frame Review	Next Frame Predict	MuirBench	LEGO-Puzzles
\checkmark			60.8	39.0
	\checkmark		61.7	38.0
		\checkmark	61.6	41.1
\checkmark	\checkmark		62.5	40.3
\checkmark		\checkmark	62.2	40.3
	\checkmark	\checkmark	62.2	39.1
\checkmark	\checkmark	\checkmark	63.8	42.3

445
 446 presented in Table 4. The findings reveal a clear synergistic effect. While each task component
 447 individually improves baseline performance, their pairwise combinations yield further gains. A
 448 model trained on the complete dataset integrating all three tasks ultimately achieves the highest
 449 performance. This confirms that the diversity of these complementary reasoning skills is crucial for
 450 fostering a comprehensive and robust understanding of temporal and procedural logic.

451 **Efficacy of Negative Samples.** A core design choice in TPRU is the inclusion of negative samples,
 452 which are instances with deliberate procedural inconsistencies that force the model to reject
 453 all options. An ablation study confirms their impact. As illustrated in Figure 4a, training without
 454 these negative samples significantly degrades performance on temporal reasoning benchmarks like
 455 LEGO-Puzzles and MuirBench. This result validates our hypothesis that teaching a model to ex-
 456 plicitly reject invalid logic is critical for advancing from pattern recognition to robust procedural
 457 understanding.



471 Figure 4: Ablation analysis. (a) Ablation on negative samples. (b) and (c) show the performance
 472 with different training samples.

473
 474 **Impact of Data Volume.** We evaluated training on data subsets up to the full 24,750 samples. As
 475 shown in Figures 4b and 4c, performance on MuirBench and LEGO-Puzzles improves with data size
 476 but begins to plateau near the full set. This pattern of diminishing returns indicates our dataset is
 477 sufficiently comprehensive to instill robust temporal understanding without requiring further scaling.

478
 479 **Impact of Training Strategy.** To validate the necessity of our Reinforcement Learning framework,
 480 we conducted a direct comparison between the proposed GRPO approach and standard Supervised
 481 Fine-Tuning (SFT). Both experiments were performed using the Qwen2.5-VL-7B backbone under
 482 consistent hyperparameters via the LLaMA-Factory framework Zheng et al. (2024). As shown in
 483 Table 5, while SFT provides a solid performance baseline, GRPO consistently achieves superior
 484 results across all benchmarks. These results indicate that GRPO is more effective than SFT for
 485 this domain, as it moves beyond simple pattern imitation to better cultivate the advanced reasoning
 486 capabilities required for complex procedural multi-modal tasks.

486
487 Table 5: Ablation study on training paradigms. We compare the performance of standard Supervised
488 Fine-Tuning (SFT) against our GRPO approach using the Qwen2.5-VL-7B backbone.
489

Training Paradigm	TPRU-Test	MuirBench	LEGO-Puzzles
Supervised Fine-Tuning (SFT)	72.88	63.03	40.60
TPRU-7B (GRPO)	75.70	65.04	42.82

493
494 Table 6: Performance comparison with state-of-the-art Video LLMs on MuirBench, LEGO-Puzzles,
495 and TPRU-Test datasets. The “Ordering” columns denote specific subtasks requiring precise
496 sequential reasoning. Best results are highlighted in **bold**.
497

Model	MuirBench		LEGO-Puzzles		TPRU-Test
	Overall	Ordering	Overall	Ordering	
LLaVA-Video-Qwen2-7B	37.88	15.63	31.91	1.0	38.61
LLaVA-Video-Qwen2-72B	41.81	10.94	41.64	5.0	44.03
SmolVLM2-256M-Video	27.92	21.88	28.18	0.0	17.79
SmolVLM2-500M-Video	25.92	7.8	27.27	0.0	16.92
Long-VITA-16K	53.07	17.19	34.45	2.0	39.26
Qwen2.5-Omni-7B	59.11	18.75	36.45	12.0	46.85
TPRU-7B (Ours)	65.04	34.38	42.82	32.0	75.70

509 4.5 COMPARISON WITH VIDEO-TEMPORAL BASELINES

511 To further elucidate the distinction between procedural temporal understanding and general video
512 understanding, we conducted a comprehensive evaluation using several state-of-the-art Video Large
513 Language Models (Video-LLMs). We posit that while general video understanding typically focuses
514 on recognizing what events occur, procedural multi-image understanding places a greater emphasis
515 on inferring the precise sequence and consequential relationships between discrete actions.

516 We compared our TPRU-7B model against strong open-source video baselines, including LLaVA-
517 Video (Zhang et al., 2024b), SmolVLM2 (Marafioti et al., 2025), Long-VITA Shen et al. (2025), and
518 Qwen2.5-Omni (Xu et al., 2025), on the MuirBench, LEGO-Puzzles, and our TPRU-Test datasets.
519 As presented in Table 6, TPRU-7B significantly outperforms these powerful video models across all
520 three benchmarks.

521 Notably, the experimental results reveal a critical gap in current video models regarding tasks that
522 require fine-grained temporal ordering. For instance, on the MuirBench Ordering subtask, even the
523 top-performing video baseline, Qwen2.5-Omni, achieves a score of only 18.8. In contrast, TPRU-7B
524 achieves 34.38 on these respective ordering tasks.

525 These findings substantiate our core hypothesis. While general video pre-training equips models
526 with a fundamental level of temporal awareness, it is insufficient for tasks necessitating precise tem-
527 poral and procedural understanding. Our approach successfully bridges this capability gap through
528 its targeted data synthesis and training strategy designed for discrete state changes.

530 5 CONCLUSION

533 In this work, we addressed the critical failure of MLLMs in comprehending visual sequences by
534 introducing TPRU, a large-scale dataset designed to systematically teach temporal and procedural
535 logic. Our experiments show that fine-tuning with a reinforcement learning strategy on TPRU yields
536 dramatic performance gains, with TPRU-7B not only dominating its baseline but also outperforming
537 the much larger GPT-4o and generalizing strongly to benchmarks like MuirBench and LEGO-
538 Puzzles. The primary contribution of this work is the demonstration that targeted, procedurally-
539 grounded data can effectively close the reasoning gap for smaller, more efficient models, moving
the frontier of capable AI from massive systems towards practical, deployable agents.

540 **6 ETHICAL CONDUCT AND SOCIETAL IMPACT STATEMENT**
541542 This research was conducted with a steadfast commitment to ethical integrity, in strict accordance
543 with the ICLR Code of Ethics. All experimental procedures and data handling protocols comply
544 with applicable national and international laws, institutional regulations, and established ethical
545 standards.546 The data utilized in this study were sourced exclusively from publicly available, open-access
547 datasets, or were obtained with explicit and appropriate authorization from the data providers. To
548 safeguard individual privacy and ensure data security, all datasets underwent rigorous preprocessing,
549 including anonymization and the removal of personally identifiable information (PII) where
550 applicable.551 Specifically regarding the video content sourced from the “Arvin Bricks” YouTube channel, these
552 materials are utilized strictly for non-commercial, transformative academic research. Consistent
553 with practices in recent literature (Ju et al., 2025), we operate under the principle of fair use for
554 publicly available creative works governed by the Standard YouTube License. Our processing and
555 analysis of this data are conducted solely to advance scientific understanding, with no commercial
556 intent or redistribution of the original assets.557 The primary objective of this work is to contribute to the advancement of scientific knowledge. We
558 have carefully considered the potential societal impacts of our research and have found no foreseeable
559 risks of direct harm or misuse. The authors explicitly disavow any application of this work
560 for malicious or unethical purposes. Furthermore, the authors declare that there are no competing
561 financial or personal interests that could have influenced the outcomes of this research.563 **7 REPRODUCIBILITY STATEMENT**
564565 To ensure the transparency and reproducibility of our research, we provide a detailed description
566 of our methodology, datasets, and experimental setup within the main body and appendix of this
567 paper. To facilitate verification and extension of our work by the research community, all associated
568 source code, data preprocessing scripts, and necessary model files will be made publicly available
569 in a repository (e.g., GitHub) upon publication. We are committed to providing a complete set of
570 materials to foster collective progress in the academic community.572 **REFERENCES**
573574 Shuai Bai, Keqin Chen, Xuejing Liu, Jialin Wang, Wenbin Ge, Sibo Song, Kai Dang, Peng Wang,
575 Shijie Wang, Jun Tang, et al. Qwen2. 5-vl technical report. *arXiv preprint arXiv:2502.13923*,
576 2025.577 Lin Chen, Jinsong Li, Xiaoyi Dong, Pan Zhang, Yuhang Zang, Zehui Chen, Haodong Duan, Jiaqi
578 Wang, Yu Qiao, Dahua Lin, et al. Are we on the right way for evaluating large vision-language
579 models? *Advances in Neural Information Processing Systems*, 37:27056–27087, 2024.580 Xi Chen, Mingkang Zhu, Shaoteng Liu, Xiaoyang Wu, Xiaogang Xu, Yu Liu, Xiang Bai, and Heng-
581 shuang Zhao. Mico: Multi-image contrast for reinforcement visual reasoning. *arXiv preprint*
582 *arXiv:2506.22434*, 2025.583 Dima Damen, Hazel Doughty, Giovanni Maria Farinella, Sanja Fidler, Antonino Furnari, Evangelos
584 Kazakos, Davide Moltisanti, Jonathan Munro, Toby Perrett, Will Price, et al. The epic-kitchens
585 dataset: Collection, challenges and baselines. *IEEE Transactions on Pattern Analysis and Ma-*
586 *chine Intelligence*, 43(11):4125–4141, 2020.588 Haodong Duan, Junming Yang, Yuxuan Qiao, Xinyu Fang, Lin Chen, Yuan Liu, Xiaoyi Dong,
589 Yuhang Zang, Pan Zhang, Jiaqi Wang, et al. Vlmevalkit: An open-source toolkit for evaluat-
590 ing large multi-modality models. In *Proceedings of the 32nd ACM international conference on*
591 *multimedia*, pp. 11198–11201, 2024.592 Chaoyou Fu, Yi-Fan Zhang, Shukang Yin, Bo Li, Xinyu Fang, Sirui Zhao, Haodong Duan, Xing
593 Sun, Ziwei Liu, Liang Wang, et al. Mme-survey: A comprehensive survey on evaluation of
multimodal llms. *arXiv preprint arXiv:2411.15296*, 2024a.

594 Xingyu Fu, Yushi Hu, Bangzheng Li, Yu Feng, Haoyu Wang, Xudong Lin, Dan Roth, Noah A
 595 Smith, Wei-Chiu Ma, and Ranjay Krishna. Blink: Multimodal large language models can see but
 596 not perceive. In *European Conference on Computer Vision*, pp. 148–166. Springer, 2024b.
 597

598 Aaron Hurst, Adam Lerer, Adam P Goucher, Adam Perelman, Aditya Ramesh, Aidan Clark, AJ Os-
 599 trow, Akila Welihinda, Alan Hayes, Alec Radford, et al. Gpt-4o system card. *arXiv preprint*
 600 *arXiv:2410.21276*, 2024.

601 Yuheng Ji, Huajie Tan, Jiayu Shi, Xiaoshuai Hao, Yuan Zhang, Hengyuan Zhang, Pengwei Wang,
 602 Mengdi Zhao, Yao Mu, Pengju An, et al. Robobrain: A unified brain model for robotic manipu-
 603 lation from abstract to concrete. In *Proceedings of the Computer Vision and Pattern Recognition*
 604 *Conference*, pp. 1724–1734, 2025.

605

606 Dongfu Jiang, Xuan He, Huaye Zeng, Cong Wei, Max Ku, Qian Liu, and Wenhui Chen. Mantis:
 607 Interleaved multi-image instruction tuning. *arXiv preprint arXiv:2405.01483*, 2024.

608 Yiming Ju, Jijin Hu, Zhengxiong Luo, Haoge Deng, Li Du, Chengwei Wu, Donglin Hao, Xinlong
 609 Wang, Tengfei Pan, et al. Ci-vid: A coherent interleaved text-video dataset. *arXiv preprint*
 610 *arXiv:2507.01938*, 2025.

611

612 Feng Li, Renrui Zhang, Hao Zhang, Yuanhan Zhang, Bo Li, Wei Li, Zejun Ma, and Chunyuan Li.
 613 Llava-next-interleave: Tackling multi-image, video, and 3d in large multimodal models. *arXiv*
 614 *preprint arXiv:2407.07895*, 2024.

615 Junnan Li, Dongxu Li, Silvio Savarese, and Steven Hoi. Blip-2: Bootstrapping language-image
 616 pre-training with frozen image encoders and large language models. In *International conference*
 617 *on machine learning*, pp. 19730–19742. PMLR, 2023.

618

619 Ziyu Liu, Tao Chu, Yuhang Zang, Xilin Wei, Xiaoyi Dong, Pan Zhang, Zijian Liang, Yuanjun Xiong,
 620 Yu Qiao, Dahua Lin, et al. Mmdm: A multi-turn multi-image dialog understanding benchmark
 621 and instruction-tuning dataset for lmlms. *Advances in Neural Information Processing Systems*, 37:
 622 8698–8733, 2024.

623

624 Quanfeng Lu, Wenqi Shao, Zitao Liu, Fanqing Meng, Boxuan Li, Botong Chen, Siyuan Huang,
 625 Kaipeng Zhang, Yu Qiao, and Ping Luo. Gui odyssey: A comprehensive dataset for cross-app gui
 626 navigation on mobile devices. *arXiv preprint arXiv:2406.08451*, 2024.

627

628 Andrés Marafioti, Orr Zohar, Miquel Farré, Merve Noyan, Elie Bakouch, Pedro Cuenca, Cyril Za-
 629 kka, Loubna Ben Allal, Anton Lozhkov, Nouamane Tazi, et al. Smolvlm: Redefining small and
 630 efficient multimodal models. *arXiv preprint arXiv:2504.05299*, 2025.

631

632 Manolis Savva, Abhishek Kadian, Oleksandr Maksymets, Yili Zhao, Erik Wijmans, Bhavana Jain,
 633 Julian Straub, Jia Liu, Vladlen Koltun, Jitendra Malik, et al. Habitat: A platform for embodied
 634 ai research. In *Proceedings of the IEEE/CVF international conference on computer vision*, pp.
 9339–9347, 2019.

635

636 Zhihong Shao, Peiyi Wang, Qihao Zhu, Runxin Xu, Junxiao Song, Xiao Bi, Haowei Zhang,
 637 Mingchuan Zhang, YK Li, Yang Wu, et al. Deepseekmath: Pushing the limits of mathemati-
 638 cal reasoning in open language models. *arXiv preprint arXiv:2402.03300*, 2024.

639

640 Yunhang Shen, Chaoyou Fu, Shaoqi Dong, Xiong Wang, Yi-Fan Zhang, Peixian Chen, Mengdan
 641 Zhang, Haoyu Cao, Ke Li, Shaohui Lin, et al. Long-vita: Scaling large multi-modal models to 1
 642 million tokens with leading short-context accuracy. *arXiv preprint arXiv:2502.05177*, 2025.

643

644 Yingjin Song, Yupei Du, Denis Paperno, and Albert Gatt. Burn after reading: Do multimodal
 645 large language models truly capture order of events in image sequences? *arXiv preprint*
 646 *arXiv:2506.10415*, 2025.

647

Kexian Tang, Junyao Gao, Yanhong Zeng, Haodong Duan, Yanan Sun, Zhenning Xing, Wenran Liu,
 648 Kaifeng Lyu, and Kai Chen. Lego-puzzles: How good are mllms at multi-step spatial reasoning?
 649 *arXiv preprint arXiv:2503.19990*, 2025.

648 Fei Wang, Xingyu Fu, James Y Huang, Zekun Li, Qin Liu, Xiaogeng Liu, Mingyu Derek Ma,
 649 Nan Xu, Wenxuan Zhou, Kai Zhang, et al. Muirbench: A comprehensive benchmark for robust
 650 multi-image understanding. *arXiv preprint arXiv:2406.09411*, 2024.

651 Peijie Wang, Zhong-Zhi Li, Fei Yin, Dekang Ran, and Cheng-Lin Liu. Mv-math: Evaluating mul-
 652 timodal math reasoning in multi-visual contexts. In *Proceedings of the Computer Vision and*
 653 *Pattern Recognition Conference*, pp. 19541–19551, 2025a.

654 Xiaochen Wang, Heming Xia, Jialin Song, Longyu Guan, Yixin Yang, Qingxiu Dong, Weiyao Luo,
 655 Yifan Pu, Yiru Wang, Xiangdi Meng, et al. Beyond single frames: Can lmms comprehend tem-
 656 poral and contextual narratives in image sequences? *arXiv preprint arXiv:2502.13925*, 2025b.

657 Zifu Wang, Junyi Zhu, Bo Tang, Zhiyu Li, Feiyu Xiong, Jiaqian Yu, and Matthew B Blaschko.
 658 Jigsaw-r1: A study of rule-based visual reinforcement learning with jigsaw puzzles. *arXiv*
 659 *preprint arXiv:2505.23590*, 2025c.

660 Siwei Wu, Kang Zhu, Yu Bai, Yiming Liang, Yizhi Li, Haoning Wu, JH Liu, Ruibo Liu, Xing-
 661 wei Qu, Xuxin Cheng, et al. Mmra: A benchmark for evaluating multi-granularity and
 662 multi-image relational association capabilities in large visual language models. *arXiv preprint*
 663 *arXiv:2407.17379*, 2024.

664 xAI team. Grok-1.5 vision preview, April 2024. URL <https://x.ai/news/grok-1.5v>.

665 Jin Xu, Zhifang Guo, Jinzheng He, Hangrui Hu, Ting He, Shuai Bai, Keqin Chen, Jialin Wang, Yang
 666 Fan, Kai Dang, et al. Qwen2. 5-omni technical report. *arXiv preprint arXiv:2503.20215*, 2025.

667 Dawei Yan, Yang Li, Qing-Guo Chen, Weihua Luo, Peng Wang, Haokui Zhang, and Chunhua Shen.
 668 Mmcr: Advancing visual language model in multimodal multi-turn contextual reasoning. *arXiv*
 669 *preprint arXiv:2503.18533*, 2025.

670 Kaining Ying, Fanqing Meng, Jin Wang, Zhiqian Li, Han Lin, Yue Yang, Hao Zhang, Wenbo Zhang,
 671 Yuqi Lin, Shuo Liu, et al. Mmt-bench: A comprehensive multimodal benchmark for evaluating
 672 large vision-language models towards multitask agi. *arXiv preprint arXiv:2404.16006*, 2024.

673 Xiang Yue, Yuansheng Ni, Kai Zhang, Tianyu Zheng, Ruoqi Liu, Ge Zhang, Samuel Stevens,
 674 Dongfu Jiang, Weiming Ren, Yuxuan Sun, et al. Mmmu: A massive multi-discipline multi-
 675 modal understanding and reasoning benchmark for expert agi. In *Proceedings of the IEEE/CVF*
 676 *Conference on Computer Vision and Pattern Recognition*, pp. 9556–9567, 2024.

677 Yi-Fan Zhang, Huanyu Zhang, Haochen Tian, Chaoyou Fu, Shuangqing Zhang, Junfei Wu, Feng
 678 Li, Kun Wang, Qingsong Wen, Zhang Zhang, et al. Mme-realworld: Could your multimodal
 679 llm challenge high-resolution real-world scenarios that are difficult for humans? *arXiv preprint*
 680 *arXiv:2408.13257*, 2024a.

681 Yizhen Zhang, Yang Ding, Shuoshuo Zhang, Xincheng Zhang, Haoling Li, Zhong-zhi Li, Peijie
 682 Wang, Jie Wu, Lei Ji, Yelong Shen, et al. Perl: Permutation-enhanced reinforcement learning for
 683 interleaved vision-language reasoning. *arXiv preprint arXiv:2506.14907*, 2025.

684 Yuanhan Zhang, Jinming Wu, Wei Li, Bo Li, Zejun Ma, Ziwei Liu, and Chunyuan Li. Video
 685 instruction tuning with synthetic data. *arXiv preprint arXiv:2410.02713*, 2024b.

686 Yaowei Zheng, Richong Zhang, Junhao Zhang, Yanhan Ye, Zheyuan Luo, Zhangchi Feng, and
 687 Yongqiang Ma. Llamafactory: Unified efficient fine-tuning of 100+ language models. *arXiv*
 688 *preprint arXiv:2403.13372*, 2024.

689 Yaowei Zheng, Junting Lu, Shenzhi Wang, Zhangchi Feng, Dongdong Kuang, and Yuwen Xiong.
 690 Easyr1: An efficient, scalable, multi-modality rl training framework. [https://github.com/](https://github.com/hiyouga/EasyR1)
 691 [hiyouga/EasyR1](https://github.com/hiyouga/EasyR1), 2025.

692 Jinguo Zhu, Weiyun Wang, Zhe Chen, Zhaoyang Liu, Shenglong Ye, Lixin Gu, Hao Tian, Yuchen
 693 Duan, Weijie Su, Jie Shao, et al. Internvl3: Exploring advanced training and test-time recipes for
 694 open-source multimodal models. *arXiv preprint arXiv:2504.10479*, 2025.

702
703

A EXPERIMENTAL SETUP

704
705
706
707
708
709

Hyperparameters. We fine-tuned the Qwen2.5-VL model (Bai et al., 2025) on our TPRU dataset. Our reinforcement learning methodology was implemented using the Easy-R1 framework (Zheng et al., 2025), employing the Group-wise Preference Optimization (GRPO) algorithm (Shao et al., 2024). Key settings included KL regularization with a coefficient of 0.01 and the generation of 5 rollouts per training sample. We used the AdamW optimizer with a learning rate of 1e-6 and trained for 2 epochs on a cluster of 8 NVIDIA A800 GPUs.

710
711

Evaluation Benchmarks.

712
713
714
715
716
717
718
719
720
721
722
723
724
725
726
727
728
729
730
731
732
733
734
735
736
737
738
739
740
741
742
743
744
745
746
747
748
749
750
751
752
753
754
755

To comprehensively evaluate the performance of our model, we assessed its capabilities on a wide variety of benchmarks. To test its generalized multi-image and multimodal reasoning abilities, we selected several established public benchmarks, including MME-RealWorld-Lite (Zhang et al., 2024a) and RealWorldQA (xAI team, 2024), BLINK (Fu et al., 2024b), MMCR (Yan et al., 2025) and MMStar (Chen et al., 2024), MMTBench (Ying et al., 2024), MMMU (Yue et al., 2024), Muir-Bench (Wang et al., 2024), and LEGO-Puzzles (Tang et al., 2025). Furthermore, to specifically measure the improvements in temporal and procedural understanding, the core focus of our work. We evaluated our model on our proposed TPRU-test. To ensure a standardized and reproducible evaluation process across all benchmarks, we utilized the open-source VLMEvalKit framework (Duan et al., 2024). We also integrated our TPRU-test into this framework, allowing for a consistent and streamlined evaluation methodology for both existing and our newly proposed tasks.

723
724

B PROMPTS FOR MICRO IMAGE SEQUENCE FILTERING

725
726

System Prompt

727
728
729
730
731
732
733
734
735
736
737
738
739
740
741
742
743
744
745
746
747
748
749
750
751
752
753
754
755

You are a professional visual data analyst responsible for filtering multi-image sequences for a machine learning dataset. Your task is to ensure that each sequence meets the following strict quality and coherence standards:

730
731
732
733
734
735
736
737
738
739
740
741
742
743
744
745
746
747
748
749
750
751
752
753
754
755

1. **Continuity of Action:** The images must depict a single, continuous, and uninterrupted action or process performed by the same subject or agent.
2. **Temporal Coherence:** The sequence must have a clear and logical chronological order. The state change between consecutive frames must be discernible and sensible.
3. **Visual Quality:** All images in the sequence must be clear and free of significant blur, corruption, or distracting artifacts. The main subject and object must be clearly visible.
4. **Scene Consistency:** The background and core environment must remain consistent throughout the sequence. Changes should be due to the action itself, not abrupt scene cuts or significant camera movement.

743
744
745
746
747
748
749
750
751
752
753
754
755

User Prompt

744
745
746
747
748
749
750
751
752
753
754
755

Strictly analyze the provided image sequence based on the quality standards. Determine if it represents a high-quality, coherent, and temporally logical process.

746
747
748
749
750
751
752
753
754
755

A sequence is considered **unqualified** if any of the following are true:

747
748
749
750
751
752
753
754
755

- The images are from different, unrelated scenes or actions.
- The chronological order is illogical or indiscernible.
- The images are severely blurry, low-resolution, or contain duplicate frames.
- The change in the scene is solely due to camera panning/zooming without a meaningful action occurring.
- The main object of the action is swapped, disappears, or is completely occluded.

754
755

Does this image sequence meet all the required standards? Please provide your answer as a single word: 'Yes' or 'No'.

756 C PROMPTS FOR MODEL TRAINING
757758 **Reasoning and Output Instruction Template**
759760 You will be presented with a task involving a set of images. The specific task is described
761 in the content below. Carefully analyze the images and the specific task description provided
762 above. Your response must strictly follow the format rules below.
763764 **ANSWER FORMAT RULES**
765766 Your response format depends on the specific task presented in the content above:
767768

1. **For an Ordering Task:** If the question asks for the correct sequence of images
(labeled A, B, C, D), your answer must be a single string representing the correct
order of the labels. Do not include spaces or other characters.
2. **For a Multiple-Choice Question (MCQ):** If the question provides options (e.g.,
A, B, C, D, E), your answer must be the single letter corresponding to the correct
option. If you believe none of the options are correct, choose the letter for the "None
of the choices provided" option if available.

773 **EXAMPLES**
774775 **Example for an Ordering Task:**
776777 <think>The process starts with image C, which shows the initial state. Image A adds the
778 first component. Image B continues the process, and image D shows the final, completed
779 assembly. Therefore, the correct sequence is C, then A, then B, then D.</think>
<answer>CABD</answer>780 **Example for a Multiple-Choice Question (MCQ):**
781782 <think>The question asks to predict the state of the phone screen after tapping the 'Set-
783 tings' icon. The first image shows the home screen. Option C correctly displays the
784 main settings menu, which is the expected outcome. Options A, B, and D show irrelevant
785 screens.</think>
<answer>C</answer>786 You must enclose your reasoning process in <think> tags and your final answer in
787 <answer> tags. Output only the content within these tags, with no additional text or ex-
788 planation.
789790 D ABLATION STUDY ON DATA FROM DIFFERENT TRAINING STAGES.
791792 Table 7: Ablation study on the training stage order for the **Qwen2.5-VL-7B** model. All scores are
793 Overall Accuracy (%).
794795

Training Strategy			Benchmark Accuracy (%)	
Stage 1	Stage 2	Stage 3	MuirBench	LEGO-Puzzles
<i>Ordering</i>	<i>Next Frame Prediction</i>	<i>Previous Frame Review</i>	61.31	39.91
<i>Ordering</i>	<i>Previous Frame Review</i>	<i>Next Frame Prediction</i>	61.58	40.45
<i>Previous Frame Review</i>	<i>Ordering</i>	<i>Next Frame Prediction</i>	60.38	42.64
<i>Next Frame Prediction</i>	<i>Ordering</i>	<i>Previous Frame Review</i>	64.23	42.55
<i>Next Frame Prediction</i>	<i>Previous Frame Review</i>	<i>Ordering</i>	63.62	42.09
<i>Previous Frame Review</i>	<i>Next Frame Prediction</i>	<i>Ordering</i>	63.62	42.09
All tasks combined			65.03	42.82

805 E THE USE OF LLM
806807 During the writing and editing of this paper, the author(s) utilized Large Language Models (such
808 as ChatGPT) for text refinement to improve the clarity and accuracy of the language. These tools
809

were primarily used for grammar checking, optimizing phrasing, and enhancing readability. All core ideas, the research design, data analysis, and conclusions are the original work of the author(s). The author(s) take full responsibility for the final content of the manuscript and have carefully reviewed all AI-assisted modifications.

F TRAINING STABILITY AND REWARD ANALYSIS

F.1 TRAINING STABILITY

To demonstrate the stability of our Reinforcement Learning (RL) training process, we visualize the reward curves in Figure 5. As illustrated, the model’s average reward exhibits a rapid and smooth ascent during the initial training stages. Subsequently, the curve successfully converges to a high-score plateau and maintains stability throughout the remaining steps, showing no signs of collapse or drastic oscillations. This convergence trajectory provides strong empirical evidence that our GRPO training configuration is both stable and efficient.

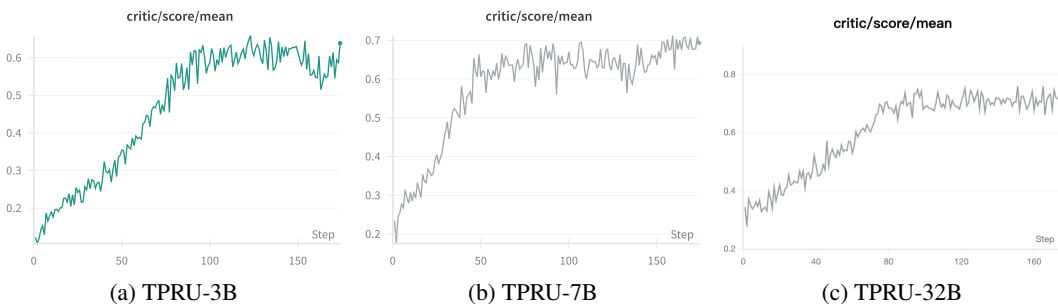


Figure 5: **RL Training Reward Curves.** The plots (a), (b) and (c) display the reward score across training steps. The curves demonstrate rapid initial convergence followed by a stable high-score plateau, indicating a stable optimization process without collapse or drastic oscillations.

F.2 ABLATION ON FORMAT REWARDS

To investigate whether the inclusion of a format-specific reward induces overfitting to the prompt structure, we conducted a dedicated ablation study. We finetuned the Qwen2.5-VL-7B without the format reward, forcing the model to learn solely from the core task accuracy reward.

As presented in Table 8, while removing the format reward results in a marginal performance decrease, the model retains robust capabilities across all benchmarks. For instance, on the TPRU-test, the performance only drops slightly from 75.70% to 74.40%. These results substantiate that the vast majority of our model’s performance stems from the acquisition of core temporal reasoning skills rather than superficial mimicry of the output format. The format reward serves as a beneficial auxiliary mechanism that enhances training stability and provides minor performance gains, but it is not the primary driver of the model’s reasoning ability.

Table 8: Ablation study on the impact of format rewards. “TPRU-7B (No-Format Reward)” denotes the model trained solely with task-accuracy rewards, excluding format-specific constraints.

Model	MuirBench		LEGO-Puzzles		TPRU-Test
	Overall	Ordering	Overall	Ordering	
TPRU-7B (No-Format Reward)	63.96	29.69	41.64	28.0	74.40
TPRU-7B (Ours)	65.04	34.4	42.82	32.0	75.70